Determination of the Angle of Attack on a Research Wind Turbine Rotor Blade Using Surface Pressure Measurements.

We would like to sincerely thank the reviewers for their time and constructive feedback. We have modified the manuscript according to your suggestions and we believe it has been significantly improved. We hope it now meets the high standards of WES journal. Please find below our answers to each of your comments. We have also provided a document where the changes are tracked (wes-2020-35-tracked_changes.pdf) and the updated version of the manuscript (wes-2020-35-Clean.pdf) with all the changes incorporated.

The referees' questions are on black, the authors' answers on blue. Additionally, the parts of the new manuscript that alludes to the comments are provided in "blue italic" for convenience.

Referee #1

L16: Please make it more clear, why is AoA a challenge? There are practical solutions to measure inflow, but is it aoa? The sentence/question should be open up for some reflections essential for the motivation. It would be great for the reader to have a (tablar) listing of available methods.

Authors answer: The first paragraph has been rewritten and is given below for convenience:

"The angle of attack (AoA) is, by definition, a 2-D concept. Nevertheless, on a wind turbine, the rotating system, i.e. a blade, is under 3-D effects such as tip and root vortices, yaw misalignment, velocity inductions, among others that render the precise determination of the AoA difficult (Shen et al., 2009). Additionally, the AoA is indirectly obtained through pressure or velocity fields, thus several uncertainties are added in its estimation. In this way, determining the local AoA on wind turbine blades remains one of the greatest aerodynamic challenges. At the same time, the determination of AoA is necessary in order to calculate the lift and drag forces over the blade, develop accurate aeroelastic models, or establish a control tool."

Henceforth the text was restructured adding new literature regarding AoA estimations, from field and wind tunnel experiments, following the structure: estimation based on probes, computational approaches, and on pressure taps. The suggestion for a table of AoA estimation methods was included and Table 1 has been added (please see answer to the next comment, too).

L31: At Risø(DTU) inflow measurements on a real turbine was conducted already in 90ties by Risø Nat. labs, and NREL around same time

Authors answer: The reviewer correctly highlights these two important contributions. We have added the following paragraph to include these campaigns and Table 1, where estimation methods of the AoA are listed:

"Several field measurements have been conducted using probes as one of the estimation methods for the AoA. Brand et al. (1997); Simms et al. (1999); Madsen et al. (1998); Maeda et al. (2005); Bak et al. (2011a) showed measurements results employing 5-hole probes from the Energy research Centre of Netherlands (ECN), The National Renewable Energy Laboratory (NREL), Technical University of Denmark (DTU), Mie University (Mie) and DanAero projects, respectively (see Table 1). Bruining and van Rooij (1997) used 3-hole probes in the Delft University of Technology (DUT) project. The upwash

correction was made based on wind tunnel measurement of static blade or airfoils representative of the studied blade section. It is remarkable that the case of the ECN exhibited better results without the upwash correction. This was assumed to be a result of the compensation effect of the downwash from the shed vorticity due to the variation of the bound circulation along the blade span (Schepers et al., 2002).”

Table 1. Angle of attack estimation methods on wind turbine rotor blades.

Contributor	Blades	Radius $[m]$	Re_c^a	On-blade tool	Estimation method
Field					
ECN[b], Brand et al. (1997)	2	13.72	1.8M[c]	5-hole probe, pressure taps	stagnation point, probe measurements, inverse BEM
DUT[b], Bruining and van Rooij (1997)	2	5	0.9M[c]	3-hole probe, pressure taps	inverse BEM, stagnation point, probe measurements, frontal pressure taps
NREL[b], Simms et al. (1999)	3	5	0.7M[c]	wind vane, 5-hole probe, pressure taps	probe measurements, stagnation point normalization, matching up C_P, inverse BEM
DTU[b], Madsen et al. (1998)	3	9.5	1M[c]	5-hole probe	probe measurements
MIE[b], Maeda et al. (2005)	3	5	0.5M[c]	5-hole probe, pressure taps	probe measurements
DanAero, (Bak et al., 2011a)	3	40	$1.5-6.1$M	5-hole probe, pressure taps, microphones	probe measurements, matching up C_P
Wind Tunnel					
MEXICO, Schepers et al. (2012)	3	2.25	0.8M[d]	pressure taps	inverse BEM, inverse free wake, based on CFD
LMEE, Sicot et al. (2008)	2	0.67	300k	pressure taps	lifting line
BeRT, Klein et al. (2018)	3	1.5	290k	3-hole probe, pressure taps	probe measurements, based on CFD
UW, Moscardi and Johnson (2016)	3	1.7	300k	5-hole probe	probe measurements

(a) Re_c: Reynolds number based on chord length at 70%R and relative inflow velocity. (b) Additional information can be found on the International Energy Agengy (IEA) Annexes reported by Schepers et al. (1997) and Schepers et al. (2002). (c) Summarized in the IEA Annexes reported by Schepers et al. (2002). (d) Reported by Schepers and Schreck (2019).

L46: it depends on the blade length and scaling; a 20mm pitot tube in comparison with a 60m blade- please adjust this against wind tunnel testing

Authors answer: This sentence was rewritten: being explicit that this is relevant in the case of small test turbine models, where this dimensions are comparable:

“In general, according to the published literature, external probes can be used to determine the AoA. However, in the case of wind turbine models, such probes are intrusive and significantly disturb the flow over the blade section where are mounted.”

L48: no references given

Authors answer: This general statement is now followed by several citations regarding each research that employs surface pressure data.

"Other complementary tools, used on research turbines are surface pressure sensors, located along the blade chord. These sensors are used to record the pressure distribution along the blade chord at a desired radial position and to calculate the aerodynamic loads. Different computational methods use this information has a source to estimate the AoA.

The inverse BEM method is probably the most common. From the surface pressure sensors, the normal and tangential forces are calculated. Assuming that they are uniform over an annulus containing the blade section. The wake-induced velocities are calculated according to momentum theory, yielding the effective velocity vector and subsequently the AoA (Whale et al., 1999). This method was implemented by ECN, NREL, DTU projects, obtaining similar results with their respective probes estimations.

Schepers et al. (2012) presented the inverse free wake method applied to the MEXICO rotor, which follows the same BEM principle but using the normal and tangential forces into a free wake model. Several computational methods can be found in the latest phase of the project, summarized by Schepers et al. (2018), such as azimuth average, three point and lifting line average methods among others.

The surface pressure measurements also allow experimental estimations. Shipley et al. (1995) showed the stagnation point normalization method described as follows: the local dynamic pressure is estimated as the maximum value of the pressure side in each pressure distribution station. This value is used to estimated the freestream velocity and then the AoA based on the geometrical velocities defined by pitch, yaw and azimuth angles.

Moreover, Brand (1994) presented the stagnation point method. The AoA is estimated as follows: The stagnation point is located as the previous method. Afterwards, the intersection of the chord line and a line normal to the surface at the stagnation point is used to estimate AoA. The position of the point of intersection can be determined 2D approaches either codes or wind tunnel measurement (Whale et al., 1999). The drawback of this method is that it relies only in the geometry of the blade section, assuming AoA and Reynolds number no influence.

Furthermore, Bruining and van Rooij (1997) exposed an additional method that use two frontal pressure taps, one on the pressure side and one on the suction side, working as an built-in probe in the blade. The drawback of this is that requires calibrating the blade station where the taps are located.

Schepers et al. (2002) reported the comparison between experimental probes, pressure taps and inverse BEM methods regarding the field measurement from ECN, NREL, DUT, DTU and Mie. The main conclusions found were: (1) The ambiguity of the 3D AoA definition implies that any check on accuracy can only be carried out with an arbitrary reference. (2) Before stall, the estimations of the AoA remain with differences below 1°. (3) Above stall conditions, the differences between methods can go up 4°. Table 1 shows field and wind tunnel experiments with the most common estimation methods mentioned above."

L51: unclear sentence: With a pitot pressure sensor, you know the position geometrically.

Authors answer: This paragraph has been removed because the wording was confusing. Probes and pressure taps topics are now addressed in separate parts of the literature to improve the text structure.

Figure 2 is missing definitions (Ut, Un, Urel), as well as t/n

Authors answer: This is now included in the caption on the Figure. Additionally, they are in the list of symbols

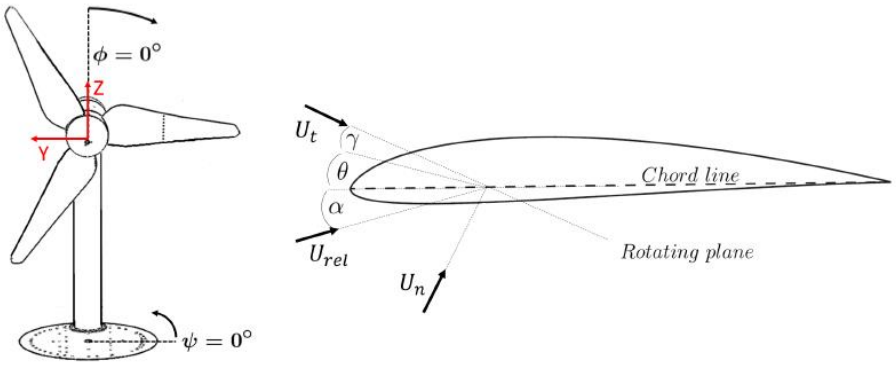

Figure 3. Angles definition. Azimuth, ϕ and yaw, ψ (left). Angle of attack, α, pitch, θ and twist, γ. U_t, U_n and U_{rel} are the tangential, normal and relative velocities, respectively (right).

L109: explain 'on a comparable level', e.g what is the implicit effect of Turbulence (1.5%)?

Authors answer: This has been included. Additionally, Fig. 2 has been added to show the level of homogeneity of the inflow and the velocity distributions over the four relevant radial positions.

"With this level of turbulence it can be expected small variations between rotations of the turbine, which suggested includes several rotations in the measurement data.

At the same time, the inflow showed some heterogeneity, i.e. was not fully uniform as is depicted in Fig. 2 (left). Figure 2 (right) shows four axial velocity distributions over at the radial positions 45; 65; 75 and 85%R. Therefore, due to these characteristics it was decided to analyze the measurement data over small azimuth angle stations."

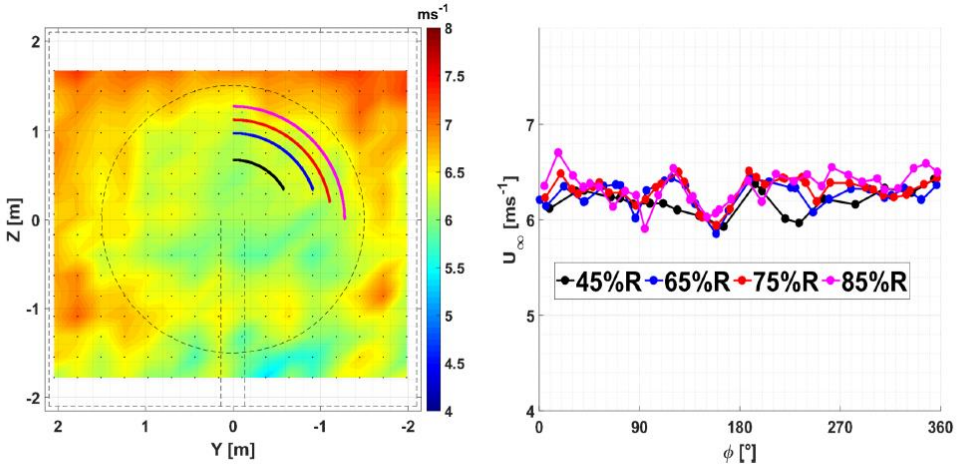

Figure 2. Axial inflow. Dashed lines: tip and tower positions. Colored lines: radial positions at 45, 65, 75 and 85%R following the blade rotation (left). Velocity distributions over radial positions at 45, 65, 75 and 85%R (right).

L118: The choice for using Clark-Y is not clear (high drag airfoil), see f. example DOI: 10.2514/6.2006-33 Conference: 44th AIAA Aerospace Sciences Meeting and Exhibit.

Authors answer: Additional information has been added (see below). Regarding the high drag values in Fig 2 (DOI: 10.2514/6.2006) Cl/Cd plot, these are for very low Reynolds number ($< 10^5$). In the present experiment, under rated conditions, the Reynolds number range is $3\ x\ 10^5$ for the radial range $1.7 \times 10^5 < Re < 3 \times 10^5$.

"A slightly modified Clark-Y airfoil profile is used along the entire blade span and there is no cylindrical root section. The airfoil modification was necessary in order to account for a realistic trailing edge thickness with respect to manufacturing requirements. Aerodynamically, the design intended to avoid stall while keep offering optimal performance and the maximum internal space to include instrumentation (Pechlivanoglou et al., 2015).

In this way, the specific airfoil profile was chosen as it performs well at low Reynolds number (Re), i.e. at the conditions relevant to BeRT (Re range from 170k to 300k along the span). The blade twist was selected so that the local AoA stays constant over the span at rated conditions"

L113: Model Blockage and consequences for interpretation of results?

Authors answer: A model to analyze the blockage effect has been implemented. This is in terms of the equivalent freestream velocity. Additionally, this is coupled with the geometrical calculations. The hypothesis that the offset in AoA, $\Delta\alpha = 2.3°$, between experimental approaches and analytical estimations (Figure 13 of the original submission given below for reference) was a consequence of the blockage is now strengthened by this correction. More changes due to the inclusion of this correction follow in the next answers to the referees' comments. Figure 15 shows the effect of considering the blockage correction on the analytical calculation.

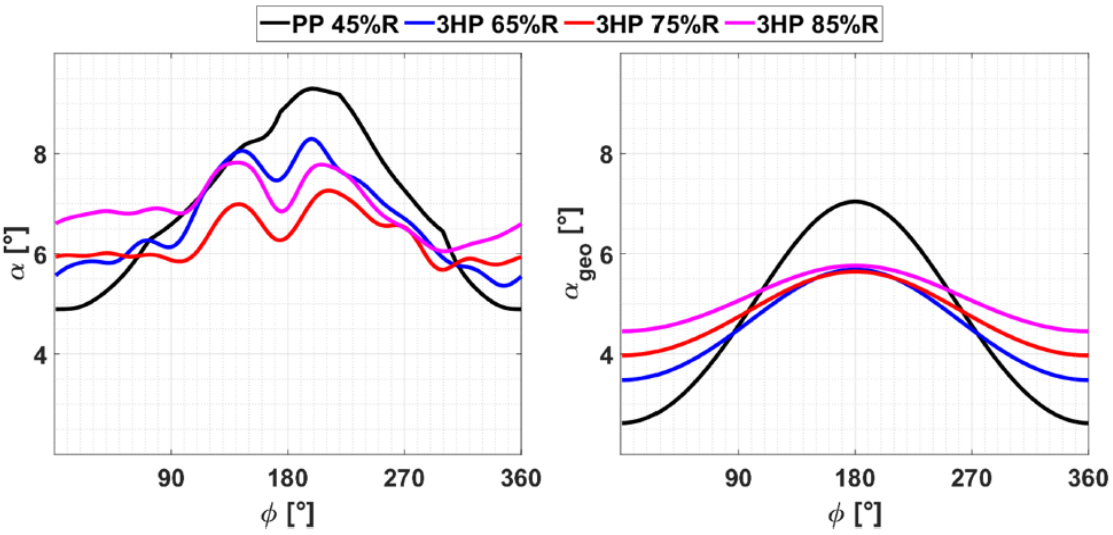

Figure 13. AoA results for yaw angle $\psi = -15°$ and pitch angle $\theta = 0°$. Pressure taps and 3-hole probe approaches (left). Analytical calculations (right).

"The turbine rotor area (A_{BeRT}) produces a considerable blockage ratio in the wind tunnel, $\epsilon = A_{BeRT}/A_{tunnel} \approx 0.4$. The blockage effect was analyzed in terms of the equivalent freestream velocity (U') which produces the same torque. Glauert (1926) showed that for a propeller the ratio between the wind tunnel velocity (U_∞) and its corresponding equivalent freestream velocity is a function of the blockage ratio and the thrust coefficient (C_T), Eq. 1. Using the BeRT rotor characteristics reported by Marten et al. (2019), a thrust coefficient of $C_T = 0.77$ (expected at rated condition) was considered. Subsequently, applying Eq. 1, implemented on wind turbines, results in the velocity ratio of U_∞/U'=0.86.

$$\frac{U_\infty}{U'} = \left(1 - \frac{\epsilon C_T}{4\sqrt{1+C_T}}\right)^{-1}$$

It is noted that this correction has also been applied successfully in wind tunnel experiments with even higher blockage ratio (45% Refan and Hangan, 2012)"

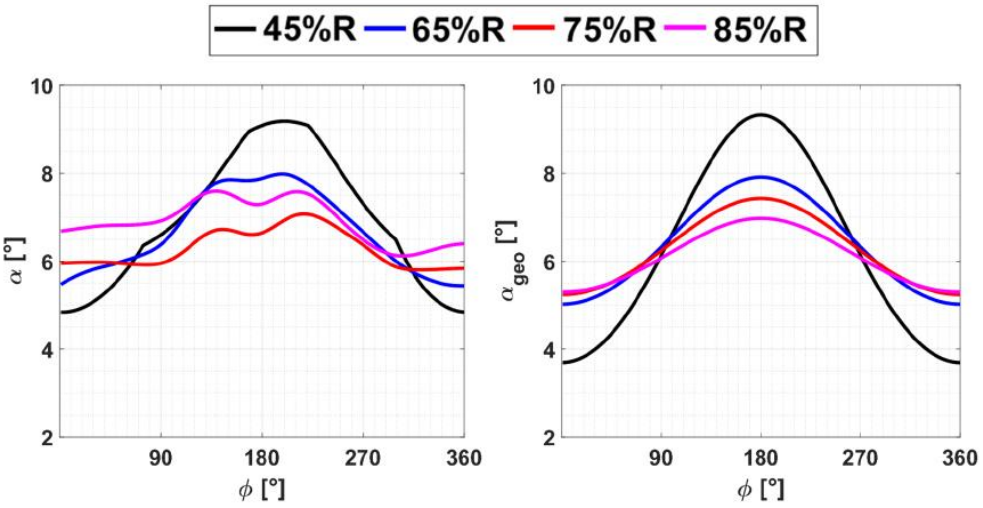

Figure 15. AoA results for yaw angle $\psi = -15°$ and pitch angle $\theta = 0°$. Pressure taps and 3-hole probe approaches (left). Analytical calculations (right).

L115: is the turbine yaw fixed or free?

Authors answer: Both the turbine yaw angle and the blade pitch angle are fixed during the measurements. The text has been rewritten:

"The turbine yaw angle and the blade pitch angle were fixed during the measurements"

L124: the statement of placement of pressure taps is not constant=0.45-why straight line placement?/why is it in this small scale experiment not following constant radius?

Authors answer: The reason is related to have good comparability with 2D airfoil studies. A drawing of the pressure taps together with the curvature (red line) is shown here. Although the curvature error is considered small (Δr<0.025 m), it was considered when the pressure was corrected by centrifugal effect as shown Eq 2.

$$P_{corr} = P_{si} + \frac{\rho}{2}(\Omega r_i)^2$$

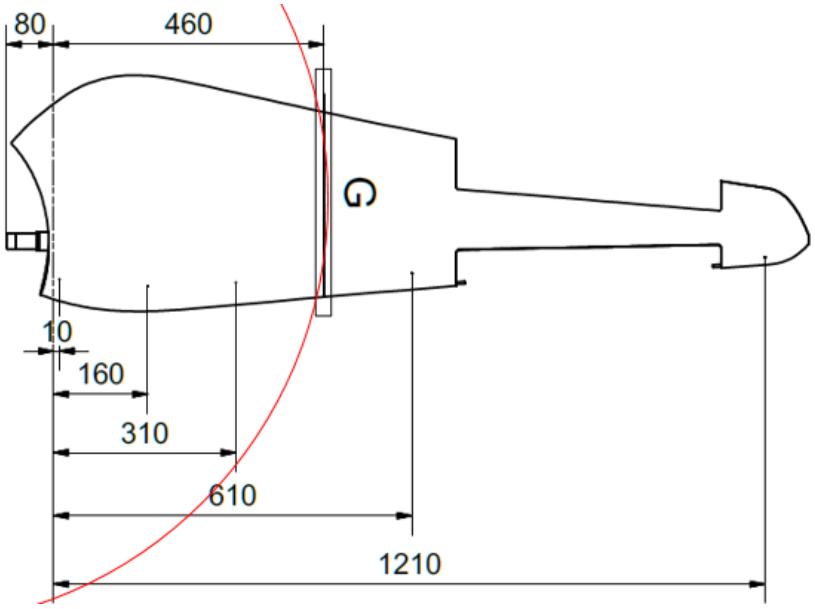

L126: what is the max frequency (3 dB limit) of the detectable signal. **L129** specs?

Authors answer: Spectra from both experimental tools (3-hole probes and pressure tap) have been included in Fig. 7.The same spectra shown in Figure 7 is presented here in [dB], the 3dB line is plotted in red with the max frequency at $\approx 6Hz$. More information regarding the filtering decisions using the spectra can be found in the following answers.

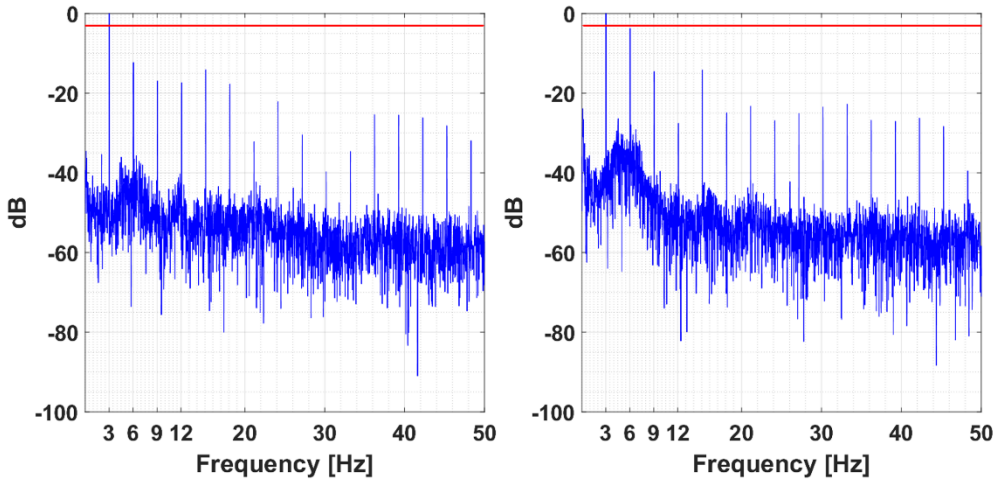

Figure 7. Frequency spectrum of one pressure sensor of the 3-hole at $75\%R$ (left). Frequency spectrum of the pressure tap at $x = 2\%c$ (right). Both cases on pitch angle $\theta = 0°$ and yaw angle $0°$

L134: A miss why the use of flaps with consensus on title /intro & science objectives

Authors answer: The TE-flaps were set in their neutral position for all the experiments, and they are given in the description only for completeness of the blade information. The sentence below explicitly states this. Additionally, the same information has been added to the caption of Figure 5.

"The flaps were fixed without any deflection for all test cases presented in this study."

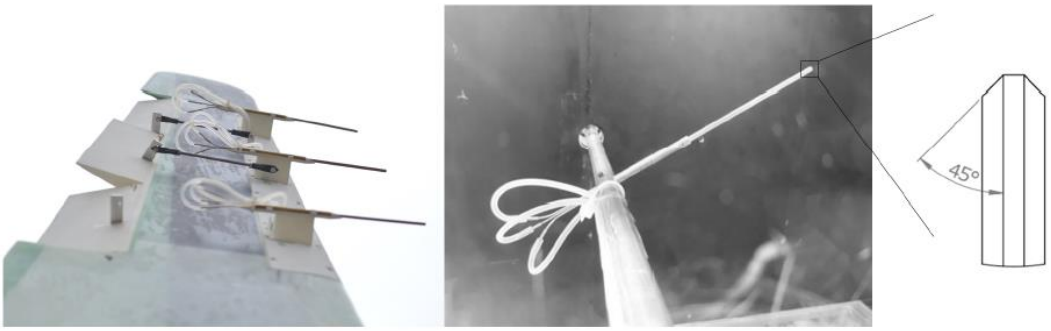

Figure 6. 3-hole probes mounted in the equipped blade (left). Calibration of a 3-hole probe and tip details (right). It is noted that although the flaps appear deflected in the photo, they were always in the neutral position for the experiments of this campaign.

L157: using a 3 hole probe-no side slip detection. What about the flow conditions when the turbine is in yaw? **L237:** the discussion of cross flow (sideslip) for the 2D probe is missing. Or may be your statement is to use a 2D probe in the 3D inflow as a representation of the normal(tangential) velocity components? Clarification and error calculation is needed. **L310:** the question is if yaw affetcs the pressure in the dynamic inflow field, observed here with a 2D-probe.

Authors answer: The effectiveness of the 2D probe over the misaligned cases has been addressed and is added here for convenience:

"As the turbine was set under yaw misalignments, it is important to verify the effectiveness of the 2D probe. The range of the AoA, in the probe stations, is $0° \leq \alpha \leq 10°$*. Therefore, adding the corresponding twist angle, the range of the AoA relative to the probes* $\alpha_{probe} \leq 18°$*. Moreover, the probes are aligned with the chord, thus the yaw angle relative to the probe is the same,* $-30° \leq \psi_{probe} \leq 0°$*.*

Zilliac (1993) and Moscardi and Johnson (2016) determined the mono-zone as $\pm 30° \left(\alpha_{probe}, \psi_{probe}\right)$*. This zone represents where the calibration parameters of the probes remain invariant, i.e.* $C_{P,probe}$*. These studies used probes with 7- and 5-holes, respectively. As a 3-hole probe sweep the same angle of these calibrations, its monozone should be the same.*

Moreover, Bruining and van Rooij (1997) employed 3-hole probes on field measurements with good agreement of the AOA, compared to inverse BEM and stagnation point methods. In addition, Klein et al. (2018) showed similar results from experimental and CFD simulations where the wind tunnel structure was considered. Therefore, based on these arguments, it was assumed that the 3-hole probes are able to estimate the AoA in the yaw misalignments here studied."

Figure 6a from Zilliac (1993) is presented here, highlighting the zone of misalignment where the current experiments were made.

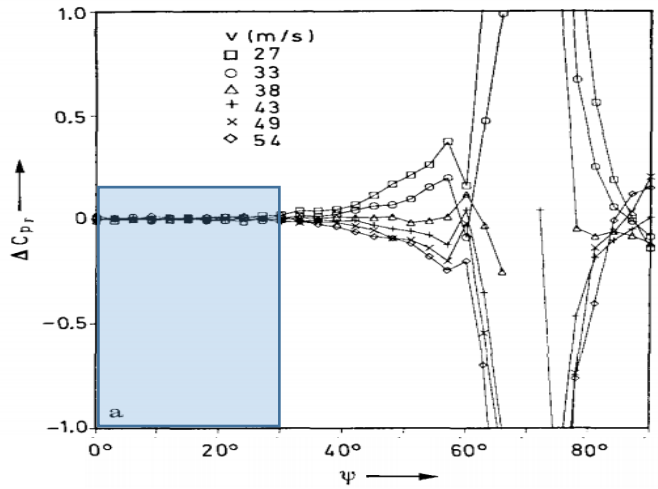

(Disclaimer: This picture does not belong to any of the authors and is presented here only as a support of the statement. Author reference: Zilliac, G.: Modelling, calibration, and error analysis of seven-hole pressure probes, Experiments in Fluids, 14, 104–120, 1993.)

L171: what is the explanation behind seeing the 1P in the signal for the interpretation?

Authors answer: The exact cause of the 1P frequency in the signal is unconfirmed at the moment. It is conceivable that it is caused by either some rotor imbalance or by the tower effect or both.

L174: This is a surprising statement about resonator box system that doesn't damp frequencies.30 Hz filter? The cited reference (Berg) offers fig 21(assuming small tubes) with considerable amplitude and phase lag properties. This needs clarification

Authors answer: The authors realize that the 30Hz filter was unsuitable, as it was higher than the structural frequencies of the blade and rotor ($f_{blade} \geq 13.5\ Hz, f_{tower} \geq 18Hz$) and also for dynamic response purposes, as the reviewer rightly highlights.

"The structural design of BeRT results in eigenfrequencies of the blades $f_{blade} \geq 13.5\ Hz$ and the tower $f_{tower} \geq 18Hz$. For this reason, the data were low pass filtered using a Butterworth filter with a cut off frequency of $12Hz$ to reduce the noise and structural vibrations."

"The dynamic response of the pressure taps/tubes system was evaluated theoretically following the model proposed by Bergh and Tijdeman (1965). Figure 8 (left) shows a scheme of the model used to apply the analysis, based on the tube arrangement depicted in Fig. 5, while Figure 8 (right) shows the theoretical response of the system, based on Bergh and Tijdeman (1965). In order to minimize the attenuation and phase lag of the signal, an additional low pass filter was applied, with a cut off frequency of $6Hz$. This was considered adequate as it shows the amplitude amplification and phase lag are less than 1% and 10°, respectively."

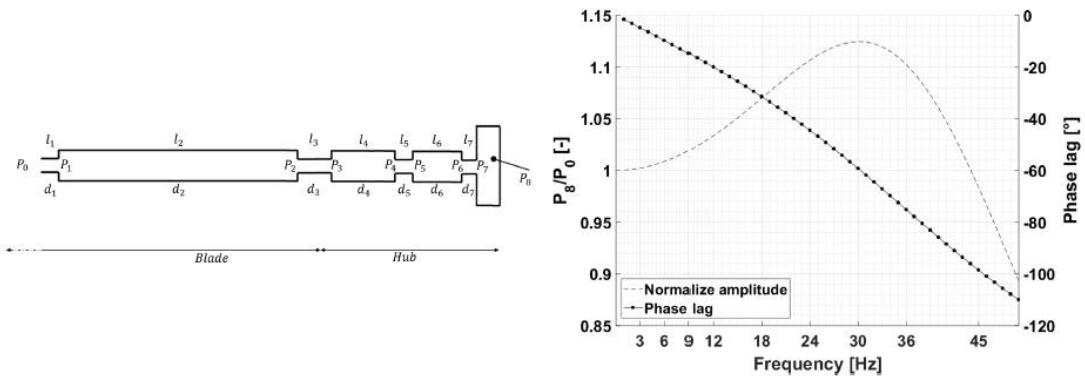

Figure 8. Scheme of the model to apply Bergh and Tijdeman (1965) dynamic response analysis, P, l and d are the pressure, length and diameter of each section (left). Theoretical dynamic response of the amplitude and phase lag (right).

To provide further insight, an additional figure is given below, where the effect of different filters is shown. Figure AA1 (left) shows the previous version, where only a low pass filter with a cut off frequency of 30Hz was used. Figure AA1 (right) shows the current results, a cut off frequency of 12 Hz in the case of the 3-hole probes and a lower cut off frequency (6Hz) for the pressure taps, in order to avoid large phase lag and damping. The two measurement tools present an improvement, reducing the vibrations and resulting in a smoother behavior.

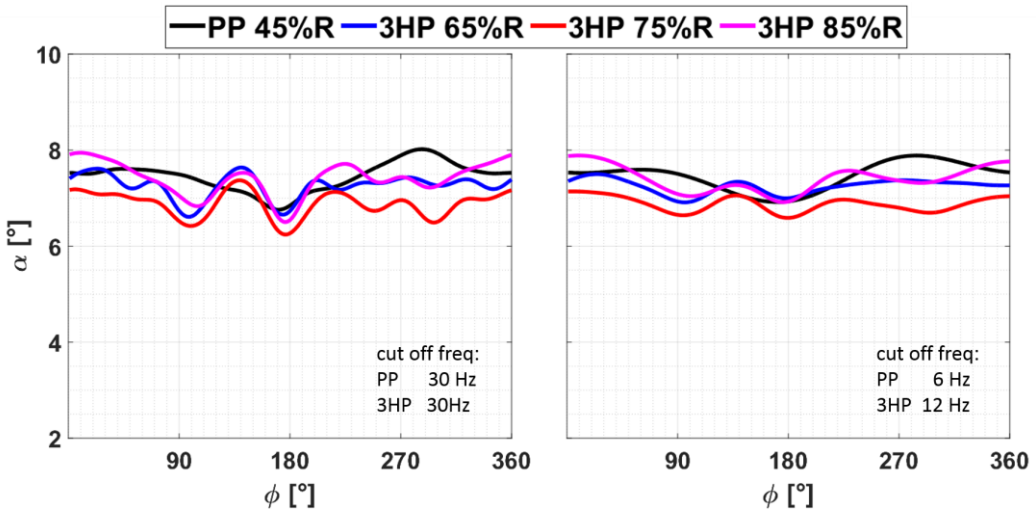

Figure AA1: AoA results from pressure taps and 3-hole probes approaches. Low pass filter with cut off frequency of 30Hz (left). Low pass filter with a cut off frequency of 12Hz and 6Hz over the 3-hole probes and pressure taps, respectively.

Figure 10: What is the difference between the black-dashed and red points around x/c=0.3..and onwards?

Authors answer: This has been included.

"The difference between both curves $\Delta C_P \leq 0.05$ until $x = 30\%c$, except the peak at the suction side ($\Delta C_P(x = 1\%c) = 0.2$). Afterwards, ΔC_P varies between $0.05 - 0.10$."

L253: temperature increases in the flow during experiments effects on the pressure sensors (standard calibration at 25deg nom)? As I recall the HCL's have +-0.25%FS nonlinearity & hysteresis. So i would assume higher uncertainty on aoa. Table1 needs to state that uncertainty is [fraction/%] of FSR

Authors answer: According to the manufacturer, the ±0.25%FS is the maximum, the nominal value is ±0.05%FS. During the experiments, the temperature range was 17.5-19.5°C. The nominal value was considered to calculate the errors.

"During the measurement campaign, between test cases, the tunnel was opened, meanwhile the changes on the pitch or yaw angle were made. This allowed to keep the temperature and relative humidity within range of $18 \pm 5°C$ *and* $40 \pm 5\%$*, respectively."*

Subsequently, the error calculation includes the nominal values, phase standard deviation and the conversion from pressure to AoA:

"The measurement uncertainty, for of all quantities, was taken into account in order to quantify the error magnitude over the results. Both AoA estimation approaches have the same iteration in the error propagation, based in the following steps:

1. Nominal error of each sensor.

2. The measurement standard deviation of the averaged measurements. This was calculated with the same azimuth step as the phase average.

3. Conversion to AoA. Thus, the error propagation after applying Eqs. 3 and 5 for the 3-hole probes and pressure taps, respectively.

Table 2 shows the overall uncertainty for all the quantities. The point 3. depends highly on the values of the measured pressure. For this reason, Table 2 shows the minimum and maximum values. An example of the uncertainty over the azimuth angle of each tool can be seen in App. D1"

It was decided to keep the units in the table to provide the uncertainty of the pressure sensors and AoAs together. An additional figure was added in the appendix (Fig D1), showing the uncertainties over each measurement tool along the azimuth angle in order to visualize their level. Here is for convenience

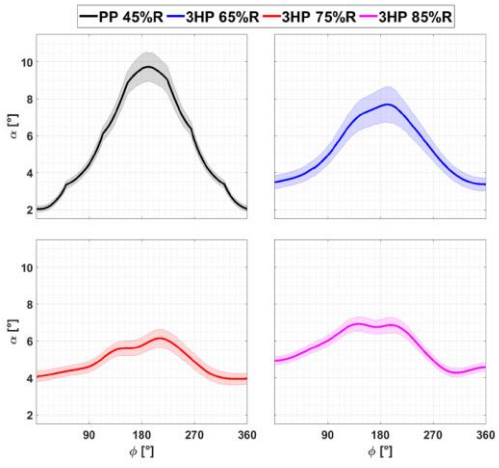

Figure D1. AoA results from the pressure tap and 3-hole probe approaches with their uncertainties. Pitch angles: $\theta = 0°$ and yaw angle $\psi = -30°$.

The figures from the section 4 of the Results were redone following the changes detailed above. The changes are regarding the new filtering

L266: The results are expressed in Pascal, may be it is more clear to show it relative (normalisation), speaking of uncertainty and also from a point of measurement range.

Authors answer: The pressure values were normalized by the dynamic pressure inflow. Consequently, the results are now non dimensional. The uncertainties described before are included in the plot and the measurement range and the level of the uncertainty on those ranges.

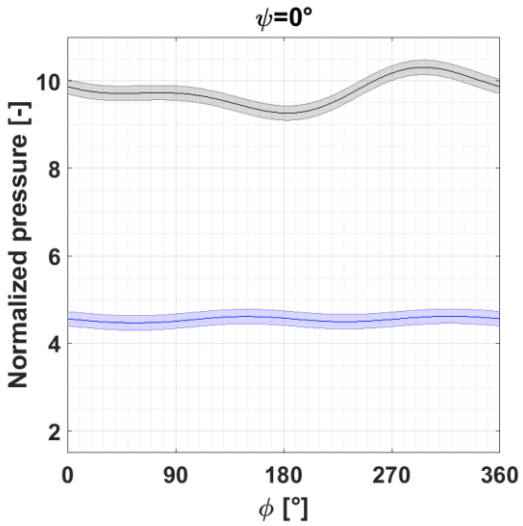

"In terms of the measurement range, the relative pressure $2.8 \leq q_{rel}/q_{\infty} \leq 6.5$ *. Over this range, the uncertainty error represents the* 4.5%*. In the case of the pressure difference at* $12{:}\,5\%c$*, the range is* $6 \leq \Delta P(12.5\%c)/q_{\infty} \leq 10.3$ *, where the error takes a value of 4%."*

Figure 14: add of result for 0 yaw missing

Authors answer: This has been included:

"Figure 13 shows the relative dynamic pressure at the radial position $r = 45\backslash\%R$ for the aligned and misaligneds cases, normalized by the dynamic pressure q_{∞}. It can be seen the same trend between the geometrical case (dashed line) and the estimation from the pressure taps (PP, solid line) as well in the maximum ($\phi = 0°$) and minimum ($\phi = 180°$) azimuth positions."

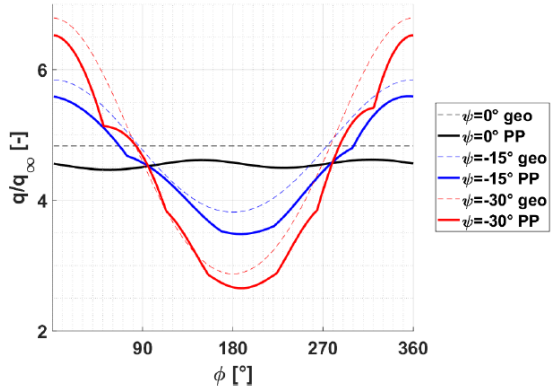

Figure 13. Normalized relative dynamic pressure at radial position $r = 45\%R$ and yaw misalignment cases of $\psi = -15°$ and $\psi = -30°$. Solid line, pressure tap estimation. Dashed line, geometrical calculation.

Figure 12 Odd, with the 2-2½P variations(L316), except for the tower influence... Check! **L334** Could this be the damping effects from the resonating tubes characteristics?, same p variation issue as above

Authors answer: The addition of the new filters and the inflow heterogeneity explain the behavior.

"The explanation is due to the heterogeneity of the inflow. These variations, $\Delta U_\infty = \pm 0.2 ms^{-1}$(see Fig. 2), can have the same influence that the tower over the AoA estimations. Using the geometrical estimation, α_{geo} , under this level of variation in the inflow, results in AoA difference of $\Delta\alpha_{geo} = \pm 0.4°$, which support this statement."

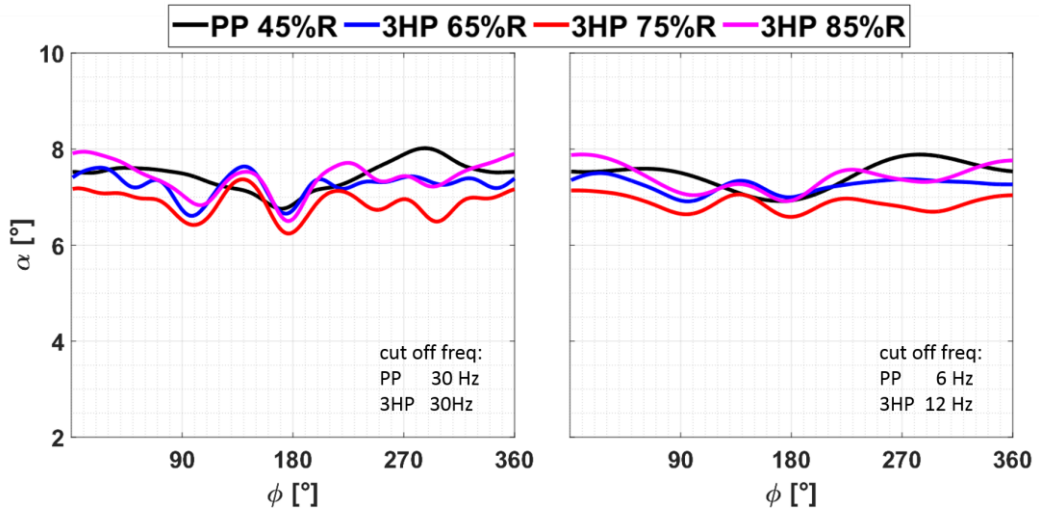

The main reason was that the filter decision in the first version, did not count the lower Eigen frequencies of the blade and tower. Also with the new filter, it seems that the vibration on the mounting of the 3-hole probes was suppressed.

Referee #2

L139: Is there a reason for this very high logging frequency?

Authors answer: The experimental set up has been designed to fulfill the requirements of active flow control with flaps. This information has not been included in the text as it is not relevant to the objective of this study.

L148: Check how the references are referenced

Authors answer: The references are now between parentheses.

"According to the BeRT design specification, the combination of chord and twist distribution achieves an optimal shape (Pechlivanoglou et al., 2015) which provides a constant AoA over most of the blade span (Bartholomay et al., 2017), so the AoA at the radial position of the pressure taps and the 3-hole probes should be the same under aligned flow conditions."

L187: Can this fit be shown and has the fit been checked with measurements from the blade at standstill? If this is possible?

Authors answer: An example of the downwash correction has been added in Eq. 4:

"*Equation 4 shows an approximation of the downwash correction (Klein et al., 2018).*

$$\alpha = 0.58°\alpha_{probe} - 0.64°$$

"

L200: Can you elaborate a little more on this? Why is it neglected and what (if any) consequences does it have?

Authors answer: Including these terms would imply additional added masses. Nevertheless, the quasi-static condition of evaluation that was applied is found enough to neglect this degree of freedom.

L227: It would be good with a comment on how good the fit is or perhaps a figure that shows the fit.

Authors answer: The coefficient of determination has been included:

"The fit values are $k_1 = 0.23$ and $k_2 = 0.43$, with a coefficient of determination of $R^2 \geq 0.999$."

L231: Why did you choose this position and not one where there were pressure taps, so you can avoid the interpolation?

Authors answer: The intention is to perform Gaunaa's method with as little modification as possible. The literature and the applied assumptions are related to this position. The introduction of alternative positions would imply a re-evaluation of all the conditions described Section 3.3.2, or create confusion on potential users. Thus, with the idea of the implementation of the method in other test rigs, it was decided to keep it.

L247: Change "Equation 7 it can..." to "Equation 7 can..."

Authors answer: Done.

Table 2 What is "FSR"?

Authors answer: FSR stands for Full Scale Range. It was changed to "Range"

L274: Rephrase the sentence, especially the part with "...to after drops..."

Authors answer: This sentence has been rewritten.

"The pressure difference at $12.5\%c$ remains relatively constant, $\Delta P(12.5\%c) = 9.8\, q_\infty$, until the azimuth angle $\phi = 90°$, to afterwards, decreasing continuously until the azimuth $\phi = 180°$ where it reaches its minimum, $\Delta P(12.5\%c) = 9.3\, q_\infty$."

L297: Rephrase the sentence. It is an important observation, but difficult to understand as it is written here.

Authors answer: This sentence has been rewritten.

"The pressure taps are located at discrete points on the blade surface. For this reason, the sensor that estimates the stagnation point, i.e. the values of the relative dynamic pressure, fluctuate in location. The latter explains the sharp changes present in yaw angle $\psi = -15°$ at azimuth angles $\phi \approx 70°$ and $\phi \approx 300°$ and yaw angle $\psi = -30°$ at azimuth angles of $\phi \approx 50°$ and $\phi \approx 320°$ (see Fig. 11)."

L303: List of symbols Missing expression for the tip speed ratio.

Authors answer: The tip speed ratio is included in the list of symbols. Also in the text, it was defined in section 3.4.

"For all cases, the tip speed ratio was fixed $\lambda = 4.35$."

Figure 15 Legend is different from Figures 16, 17 and 18. Figure 15 Perhaps repeat that AoAgeo = 5.1 deg from.

Authors answer: Done. The Analytical AoA estimation was included, to keep the same format of the misalignment cases (with the blockage correction. 5.1deg is no longer valid).

L321: Can the uncertainties be added on the figure?

Authors answer: This would overload the Figures at the section. Nevertheless, One representative Figure that includes the uncertainties is now included in the appendix, Fig D1.

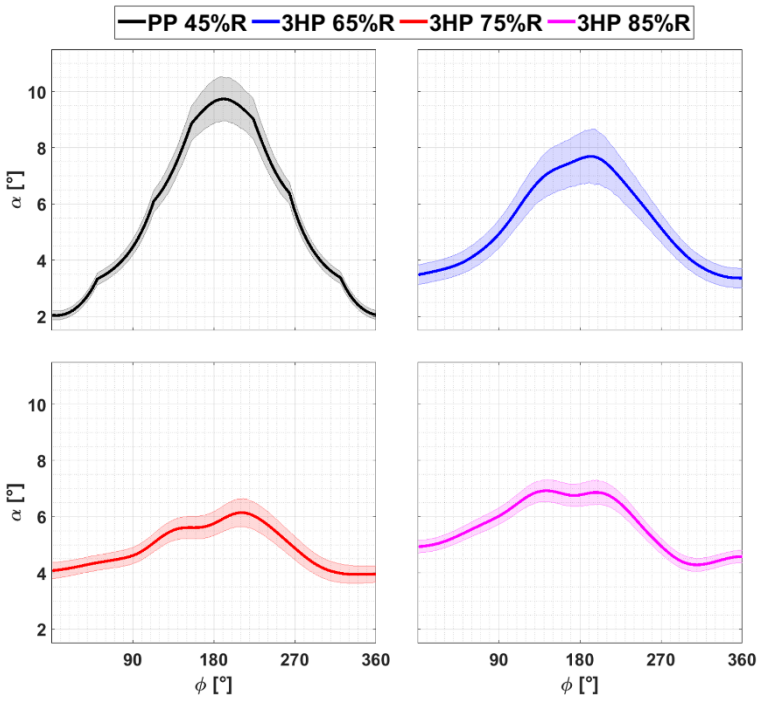

L322-23: Rephrase

Authors answer: This sentence has been rewritten.

"Although the AoA over the azimuthal variation is not constant, both methods estimate a similar AoA range. The AoA for both pressure tap and 3-hole probe methods are slightly lower than previous experimental results show by Klein et al. (2018), but within the uncertainty values. Table 3 shows the range $(\alpha_{min}, \alpha_{max})$ *and average* $(\bar{\alpha}$ *) values of the AoA over the azimuth angle for the pressure taps and the 3-hole probe methods. The range of the tools measurements is between 6.6-7.8° and the geometrical estimation between 6.4-6.8°"*

L324-26: Can the effect of the walls be quantified, e.g. by the method from H. Glauert. The elements of aerofoil and airscrew theory? Rephrase

Authors answer: A model to analyze the blockage effect has been implemented. This is in terms of the equivalent freestream velocity. Additionally, this is coupled with the geometrical calculations. The hypothesis that the offset in AoA, $\Delta\alpha = 2.3°$, between experimental approaches and analytical estimations (Figure 13 of the original submission given below for reference) was a consequence of the blockage is now strengthened by this correction. More changes due to the inclusion of this correction follow in the next answers to the referees' comments. Figure 15 shows the effect of considering the blockage correction on the analytical calculation.

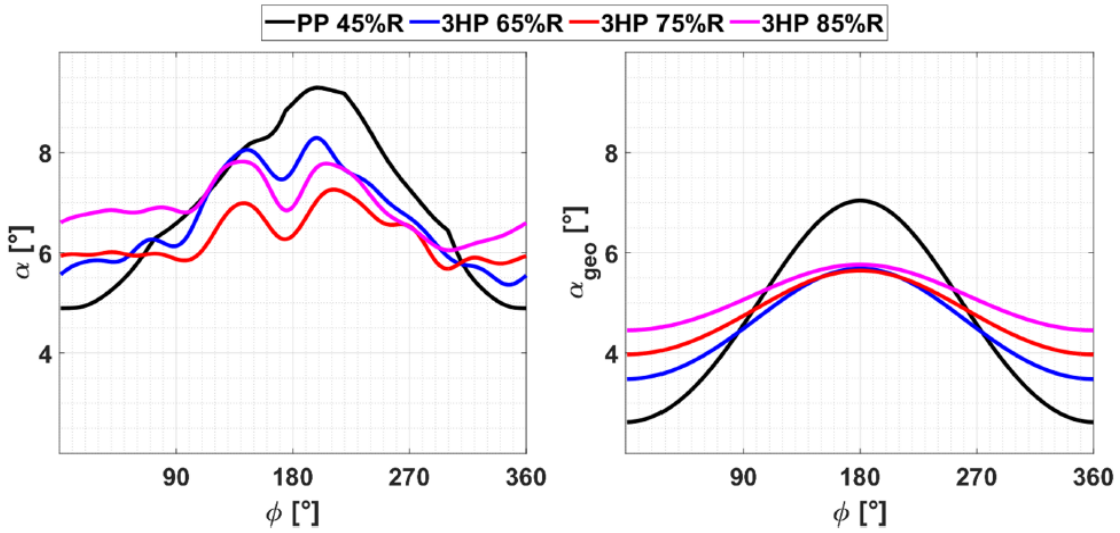

Figure 13. AoA results for yaw angle $\psi = -15°$ and pitch angle $\theta = 0°$. Pressure taps and 3-hole probe approaches (left). Analytical calculations (right).

"The turbine rotor area (A_{BeRT}) produces a considerable blockage ratio in the wind tunnel, $\epsilon = A_{BeRT}/A_{tunnel} \approx 0.4$. The blockage effect was analyzed in terms of the equivalent freestream velocity (U') which produces the same torque. Glauert (1926) showed that for a propeller the ratio between the wind tunnel velocity (U_∞) and its corresponding equivalent freestream velocity is a function of the blockage ratio and the thrust coefficient (C_T), Eq. 1. Using the BeRT rotor characteristics reported by Marten et al. (2019), a thrust coefficient of $C_T = 0.77$ (expected at rated condition) was considered. Subsequently, applying Eq. 1, implemented on wind turbines, results in the velocity ratio of U_∞/U'=0.86.

$$\frac{U_\infty}{U'} = \left(1 - \frac{\epsilon C_T}{4\sqrt{1+C_T}}\right)^{-1}$$

It is noted that this correction has also been applied successfully in wind tunnel experiments with even higher blockage ratio (45% Refan and Hangan, 2012)"

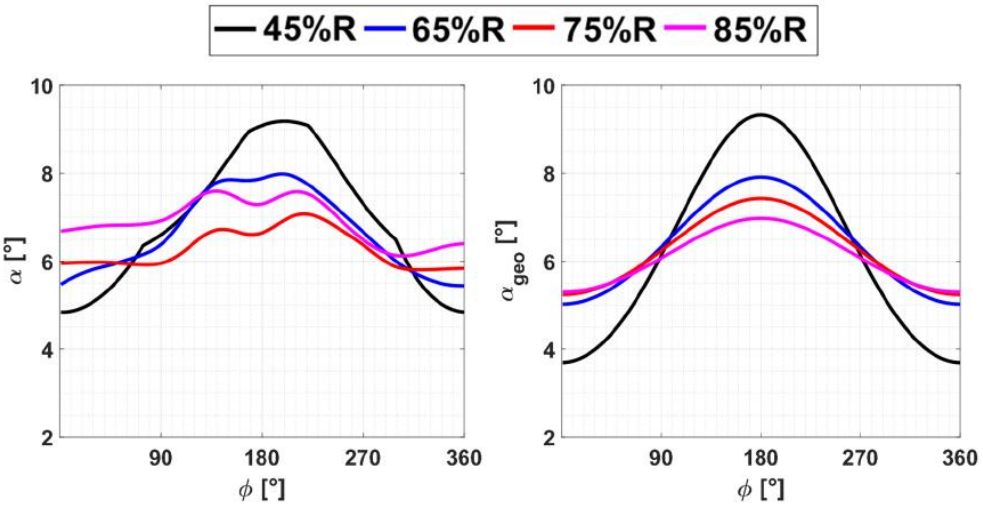

Figure 15. AoA results for yaw angle $\psi = -15°$ and pitch angle $\theta = 0°$. Pressure taps and 3-hole probe approaches (left). Analytical calculations (right).

Additionally, The method is coupled with the geometrical calculations. The hypothesis that the offset in the previous version was a consequence of the blockage was now strengthened by this correction:

"The blockage effect must be considered. Consequently, the inflow velocity (U_∞) for these calculations was replaced by the equivalent freestream velocity. Thus, applying Eq. 1 results in the equivalent freestream velocity of $U' = 7.5ms^{-1}$."

L330-31: Rephrase

Authors answer: This sentence has been rewritten.

"However, the difference is in the same magnitude of the fluctuations of each tool"

L353-56: The paragraph is unclear, please rephrase

Authors answer: This sentence was rewritten. The blockage effect was now considered, thus part of the sentence was deleted.

"The analytical AoAs, Fig. 16 (right), show the same features, including the large difference at azimuth angles $\phi = 0°$ and $\phi = 180°$"

L363: Is there an explanation on the difference in slope? Why is the measurements not showing a slope of -1? **L364** Rephrase

Authors answer: This has been included:

"Nevertheless, the induction factors change at each pitch angle, therefore the change in the slope is the results of that dependency. This agrees with the fact that the slopes are similar but not the same, as is expected variations of the induction factor along the radial positions."